

Supporting Information

Probing the morphological effects of $\text{ReO}_x/\text{CeO}_2$ catalysts on CO_2 hydrogenation reaction

Bin Yang ^{a,b,c}, Yifu Wang ^c, Longtai Li ^c, Biao Gao ^c, Lingxia Zhang ^{a,b*} and Limin Guo ^{c*}

^a School of Chemistry and Material Science, Hangzhou Institute for Advanced Study, University of Chinese Academy of Sciences, 1 Sub-lane Xiangshan, Hangzhou 310024, China;

^b State Key Laboratory of High Performance Ceramics and Superfine Microstructure, Shanghai Institute of Ceramics, Chinese Academy of Sciences, 1295 Dingxi Road, Shanghai 200050, China;

^c School of Environmental Science and Engineering, Huazhong University of Science and Technology, 1037 Luoyu Road, Wuhan 430074, China;

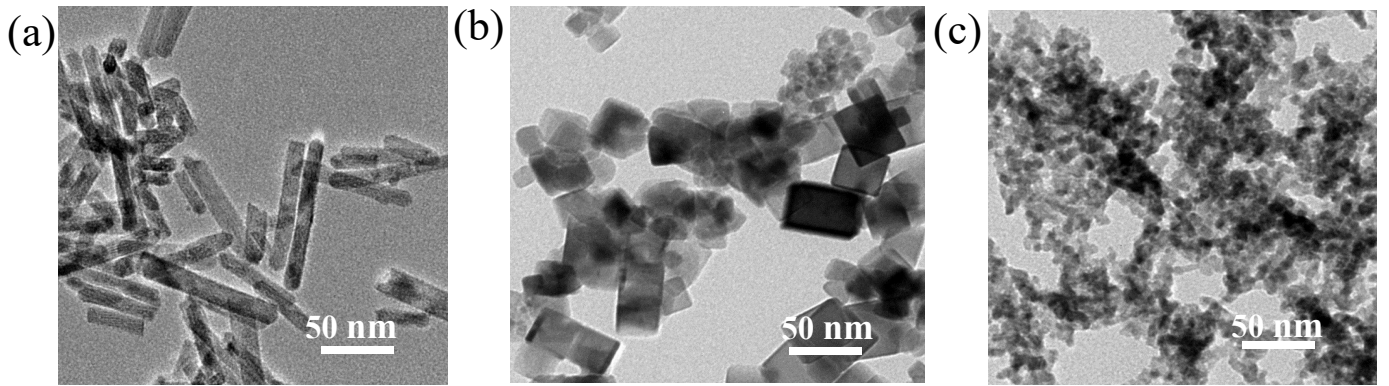


Fig. S1. HRTEM images of (a) CeO₂-R, (b) CeO₂-C and (c) CeO₂-P supports.

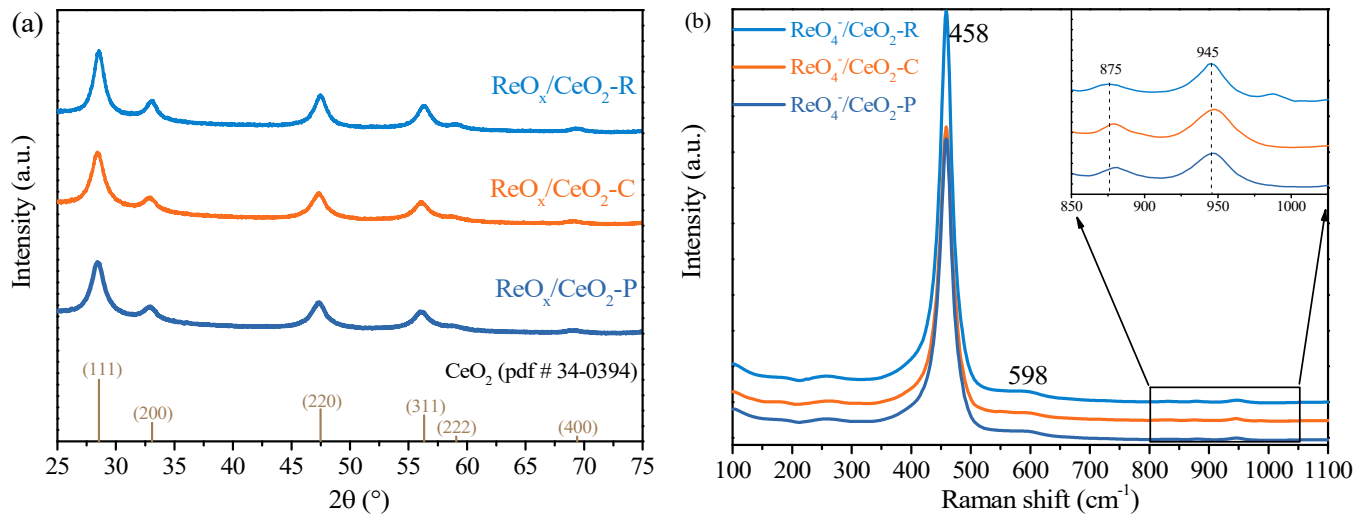


Fig. S2. (a) XRD patterns of ReO_x/CeO₂-R, ReO_x/CeO₂-C and ReO_x/CeO₂-P. (b) Raman spectra of ReO₄⁻/CeO₂-R, ReO₄⁻/CeO₂-C and ReO₄⁻/CeO₂-P.

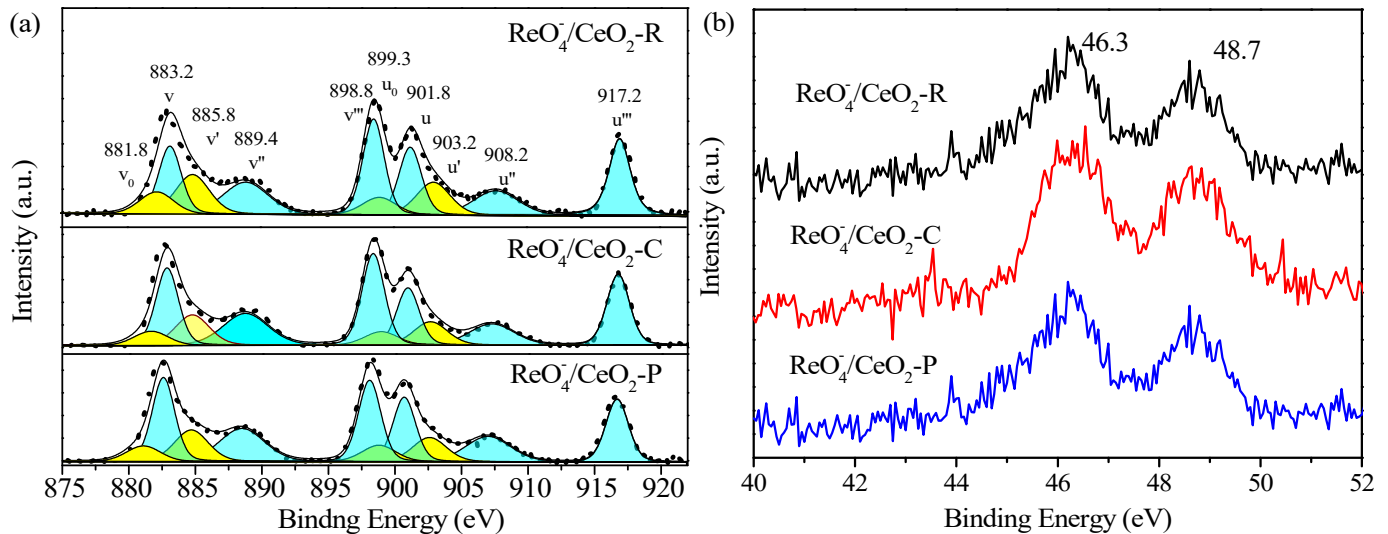


Fig. S3. Deconvolution of XPS spectra of (a) Ce 3d and (b) Re 4f of $\text{ReO}_4^-/\text{CeO}_2\text{-R}$, $\text{ReO}_4^-/\text{CeO}_2\text{-C}$ and $\text{ReO}_4^-/\text{CeO}_2\text{-P}$.

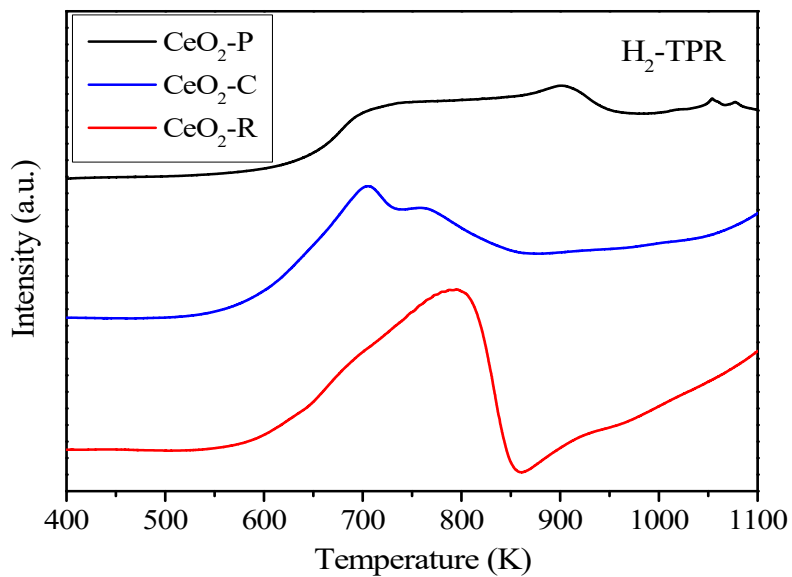


Fig. S4. H_2 -TPR of $\text{CeO}_2\text{-R}$, $\text{CeO}_2\text{-P}$ and $\text{CeO}_2\text{-C}$.

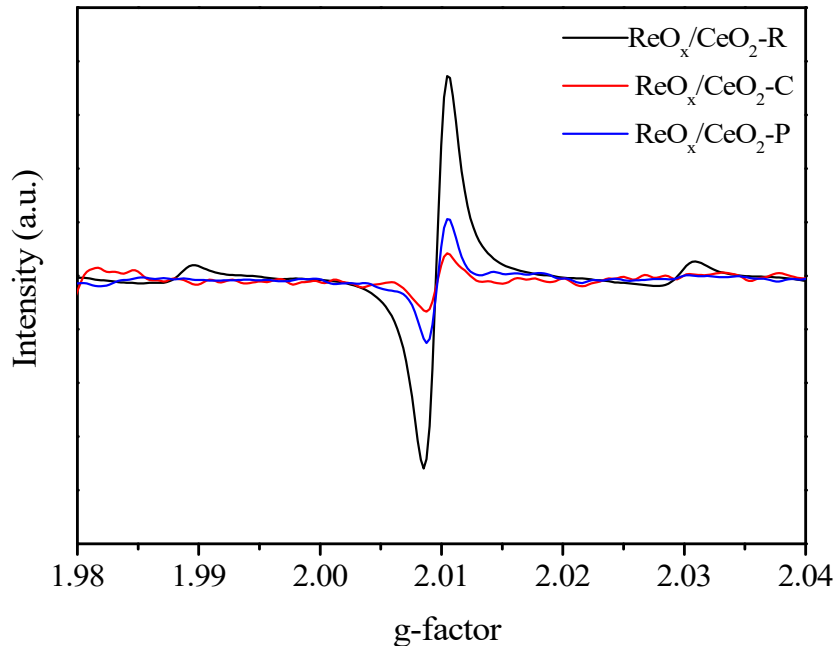


Fig. S5. EPR spectra of the catalysts.

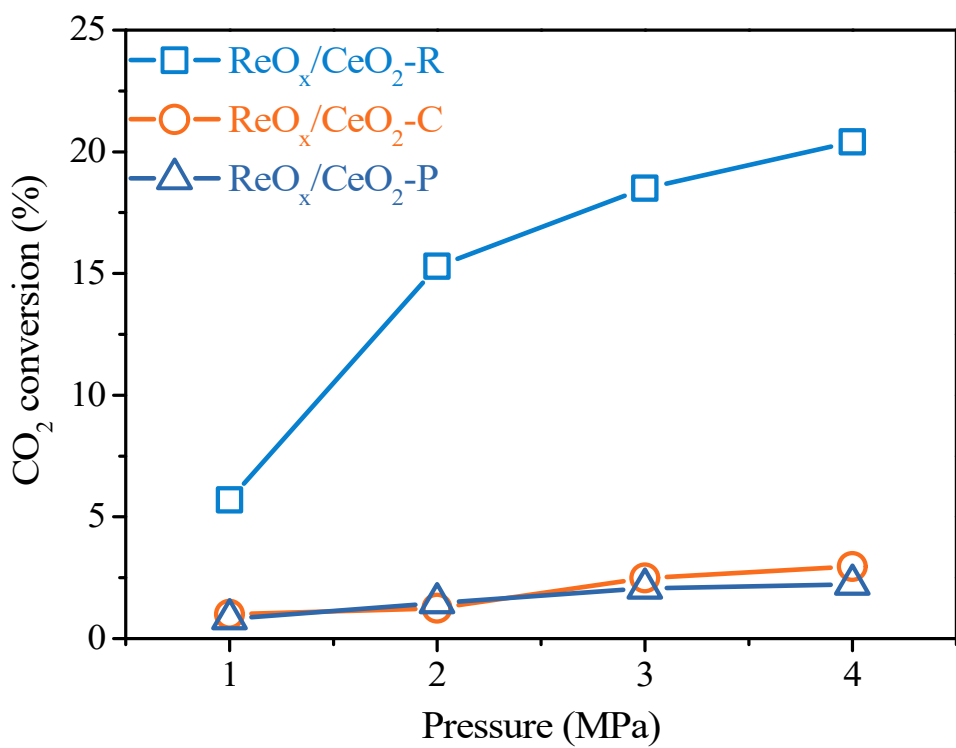


Fig. S6. The effect of pressure on CO₂ conversion on $\text{ReO}_x/\text{CeO}_2$ -R, $\text{ReO}_x/\text{CeO}_2$ -C and $\text{ReO}_x/\text{CeO}_2$ -P at 613 K, CO₂/H₂=1/3 and GHSV=12000 mL/g h.

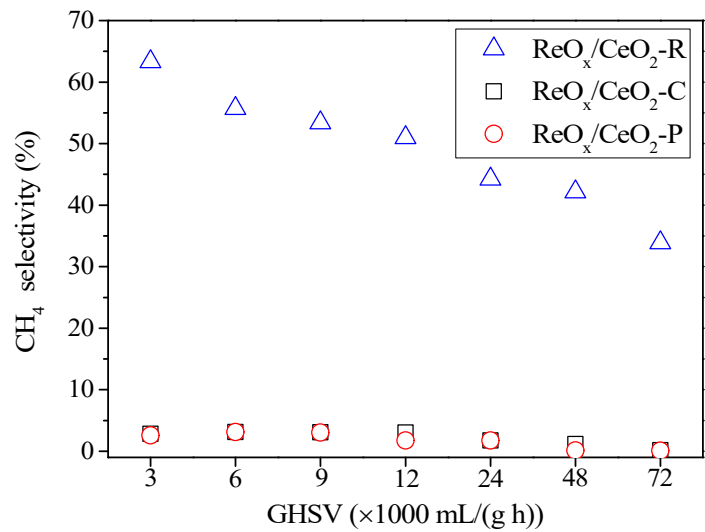


Fig. S7. The effect of GHSV on CH₄ selectivity on ReO_x/CeO₂-R, ReO_x/CeO₂-C and ReO_x/CeO₂-P at 613 K, CO₂/H₂ = 1/3 and 2 MPa.

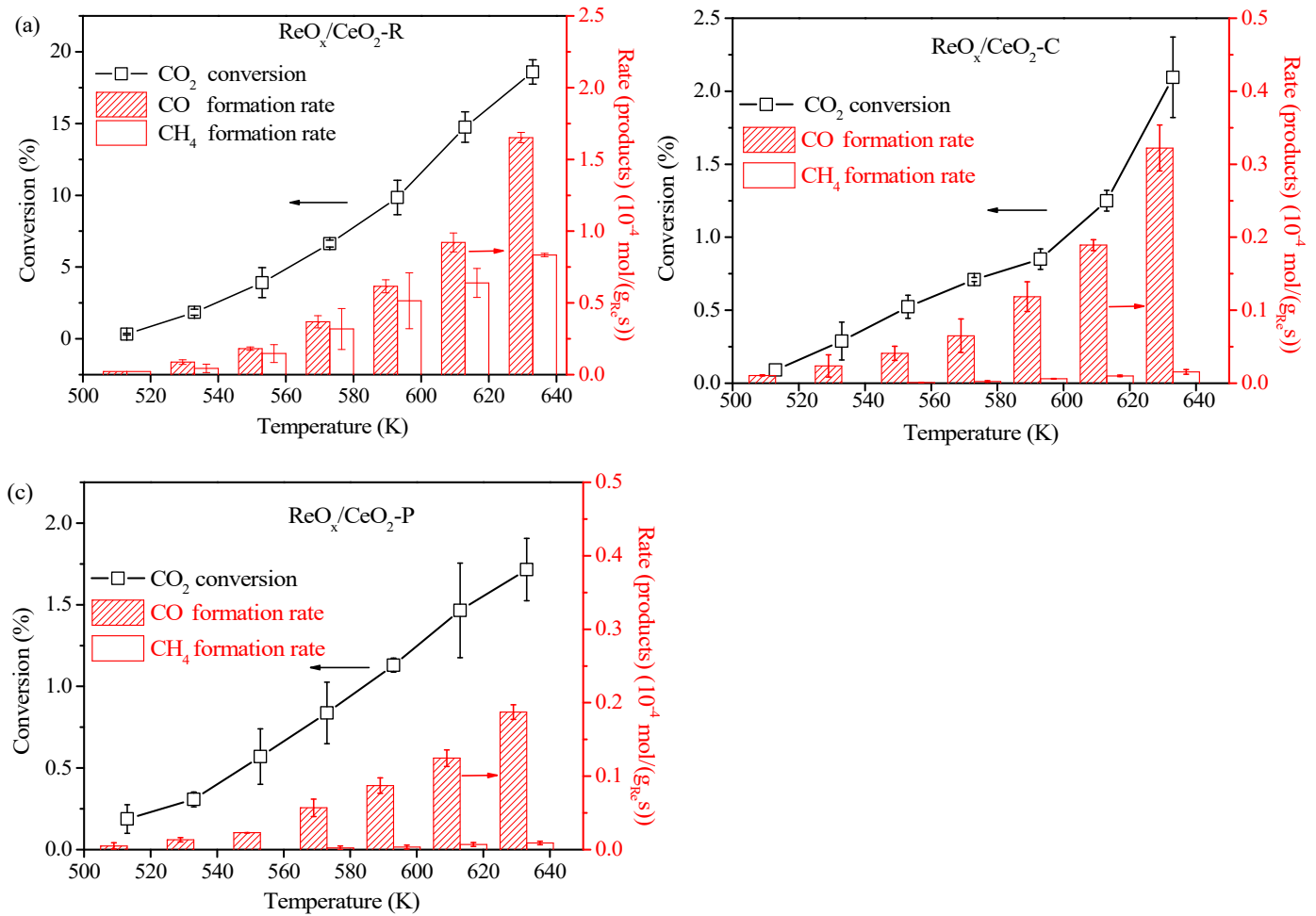


Fig. S8. Temperature-dependent performance of (a) $\text{ReO}_x/\text{CeO}_2\text{-R}$, (b) $\text{ReO}_x/\text{CeO}_2\text{-C}$ and (c) $\text{ReO}_x/\text{CeO}_2\text{-P}$. The left vertical axis is CO_2 conversion and the right is the formation rate of products.

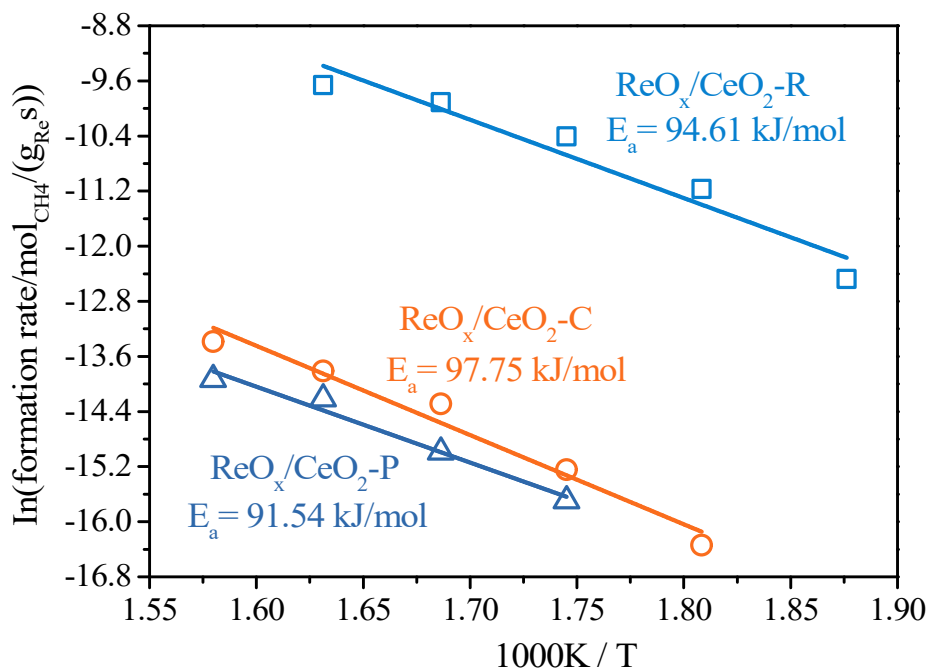


Fig. S9. Arrhenius plots for CH_4 generation on $\text{ReO}_x/\text{CeO}_2\text{-R}$, $\text{ReO}_x/\text{CeO}_2\text{-C}$ and $\text{ReO}_x/\text{CeO}_2\text{-P}$.

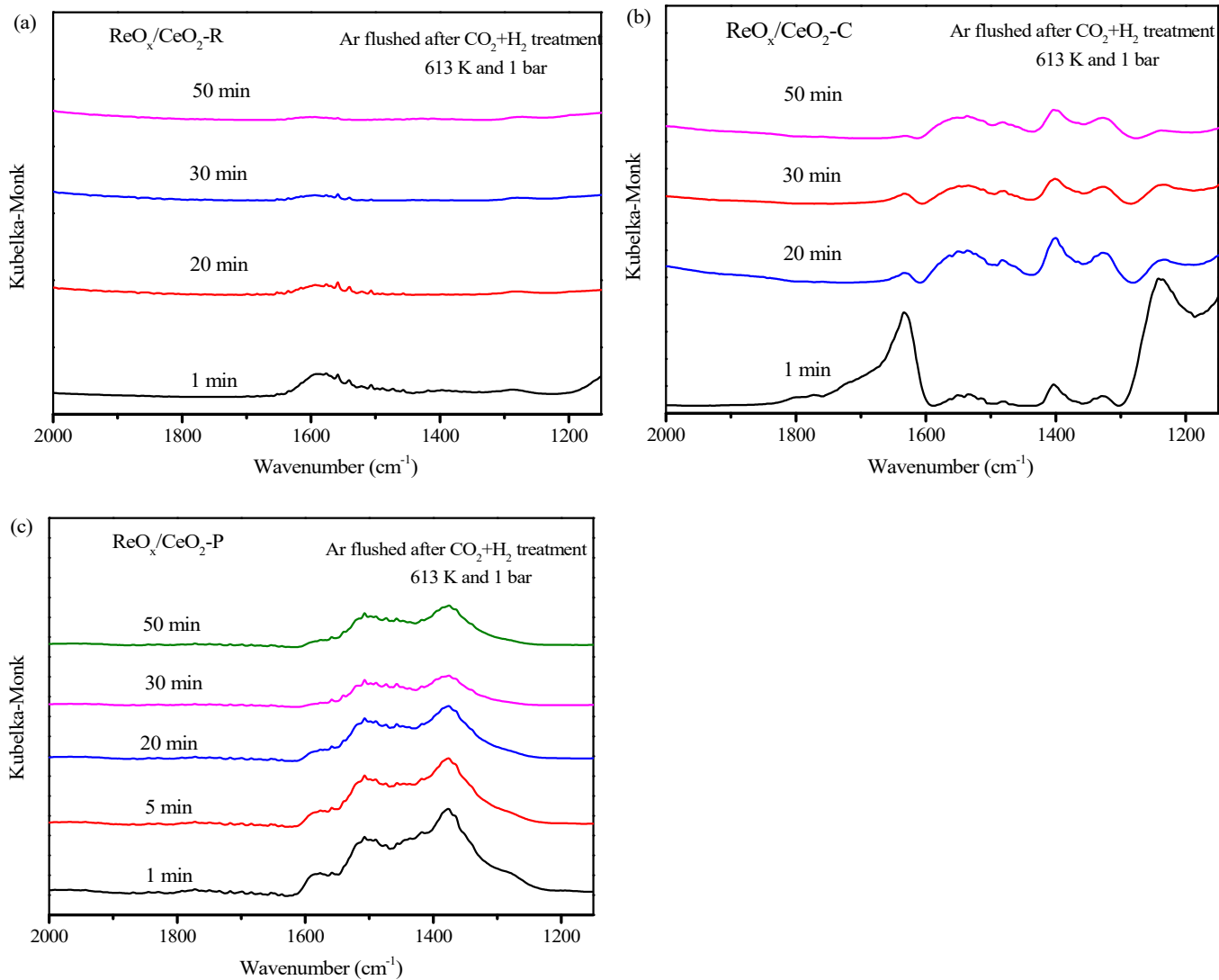


Fig. S10. Infrared spectra recorded under Ar flushing after CO_2+H_2 reaction at 633 K and 0.1 MPa. (a) $\text{ReO}_x/\text{CeO}_2\text{-R}$, (b) $\text{ReO}_x/\text{CeO}_2\text{-C}$ and (c) $\text{ReO}_x/\text{CeO}_2\text{-P}$.

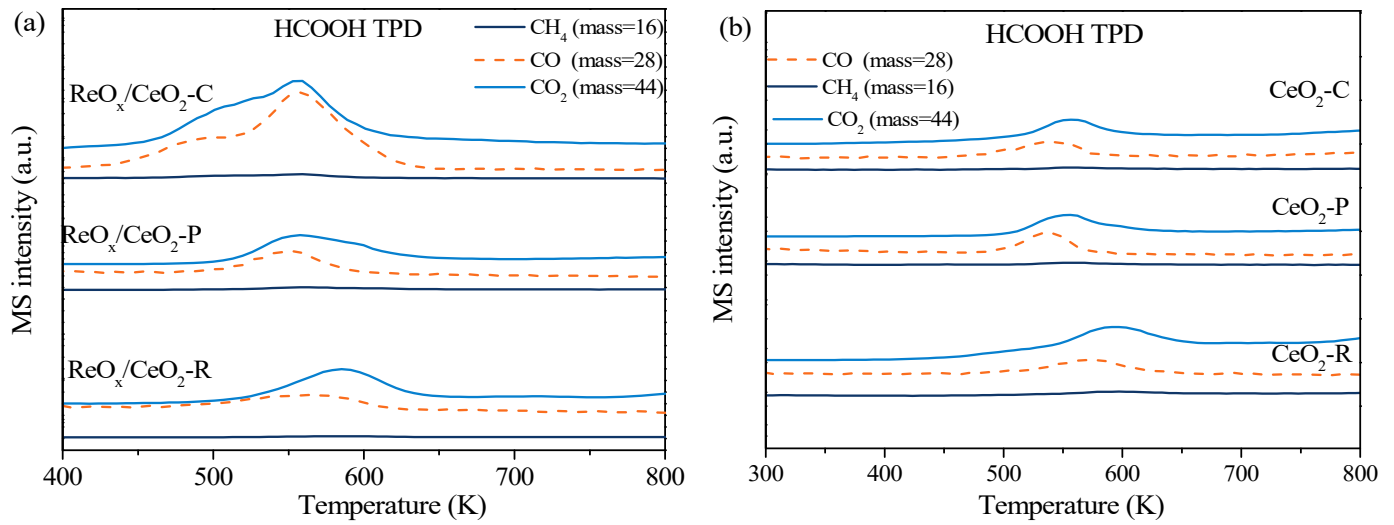


Fig. S11. TPD of HCOOH over (a) $\text{ReO}_x/\text{CeO}_2$ -C, $\text{ReO}_x/\text{CeO}_2$ -P and $\text{ReO}_x/\text{CeO}_2$ -R, (b) CeO_2 -C, CeO_2 -P and CeO_2 -R.

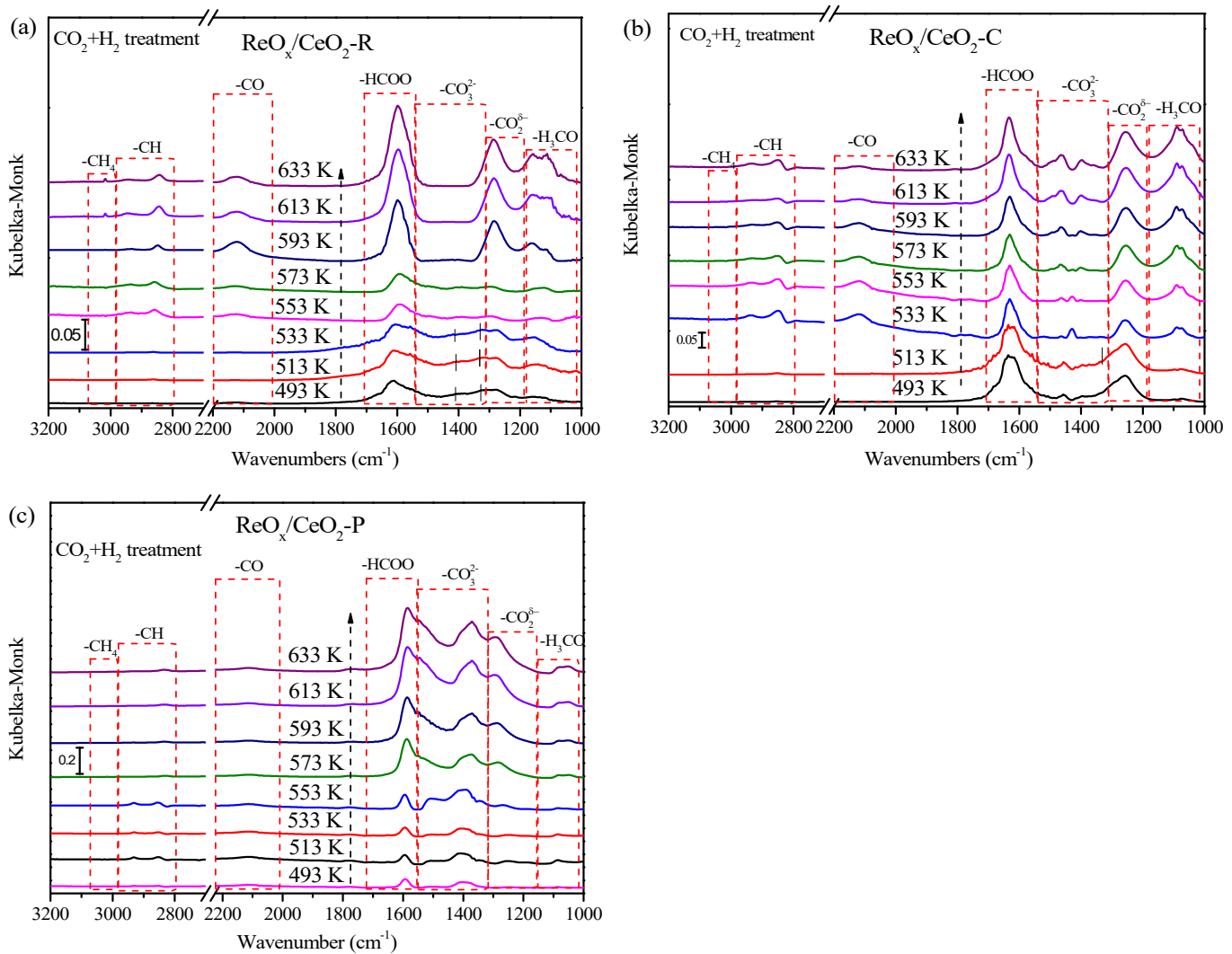


Fig. S12. Temperature-dependent infrared analysis of CO_2 hydrogenation after exposing the catalysts to CO_2+H_2 at 493 K and subsequently heating to 633 K. (a) $\text{ReO}_x/\text{CeO}_2\text{-R}$, (b) $\text{ReO}_x/\text{CeO}_2\text{-C}$ and (c) $\text{ReO}_x/\text{CeO}_2\text{-P}$.

Table S1. Assessment of extraparticle mass transfer limitations in CO₂ hydrogenation over catalysts.

Parameter	ReO _x /CeO ₂ -R			ReO _x /CeO ₂ -C.			ReO _x /CeO ₂ -P		
P(MPa)	2	2	2	2	2	2	2	2	2
T(K)	613	613	613	613	613	613	613	613	613
Particle size (μm)	25-45	25-45	25-45	25-45	25-45	25-45	25-45	25-45	25-45
W _{cat} (g)	0.05	0.1	0.2	0.05	0.1	0.2	0.05	0.1	0.2
H ₂ : CO ₂ : Ar (cm ³ /min)	36:12:2	72:24:4	144:48:8	36:12:2	72:24:4	144:48:8	36:12:2	72:24:4	144:48: 8
CO ₂ (10 ⁻⁵ mol/g _{Re} s)	14.95	15.60	15.82	1.94	1.90	2.01	1.25	1.31	1.41

Table S2. Assessment of intraparticle mass transfer limitations in CO₂ hydrogenation over catalysts.

Parameter	ReO _x /CeO ₂ -R			ReO _x /CeO ₂ -C.			ReO _x /CeO ₂ -P		
P(MPa)	2	2	2	2	2	2	2	2	2
T(K)	613	613	613	613	613	613	613	613	613
Particle size (μm)	≤25	25-45	125-300	≤25	25-45	125-300	≤25	25-45	125- 300
W _{cat} (g)	0.1	0.1	0.1	0.1	0.1	0.1	0.1	0.1	0.1
H ₂ : CO ₂ : Ar (cm ³ min ⁻¹)	72:24:4	72:24:4	72:24:4	72:24:4	72:24:4	72:24:4	72:24:4	72:24:4	72:24: 4
CO ₂ (10 ⁻⁵ mol/g _{Re} s)	15.94	15.60	15.13	1.96	1.90	1.86	1.39	1.31	1.32

Table S3. Structural parameters of the samples

	Re (wt%)-XRF	Re (wt%)-XPS	S _{BET} (m ² /g)	Pore volume (cm ³ /g)
ReO _x /CeO ₂ -R	1.97	2.21	109.06	0.32
ReO _x /CeO ₂ -C	1.98	2.02	38.24	0.16
ReO _x /CeO ₂ -P	1.98	2.31	34.39	0.19

Table S4. (1) Infrared band assignments of the surface species on ReO_x/CeO₂-C.

Surface species	Wavenumber (cm ⁻¹)	assignment
Carbonate	1398	v _s (O-C-O)
	1512	v _{as} (O-C-O)
Carboxylate	1289	v _s (O-C-O)
	2007	linearly bound
CO bond	1892	bridge bound
	2948, 2853	v(CH)
Formate	1631	v _{as} (O-C-O)
	1096	v _(CO) of terminal of bridged-OCH ₃
Methane	3019	v(CH)

(2) Infrared band assignments of the surface species on ReO_x/CeO₂-R.

Surface species	Wavenumber (cm ⁻¹)	assignment
Carboxylate	1289	v _s (O-C-O)
	2007, 1912	linearly bound
CO bond	1892	bridge bound
	2948, 2853	v(CH)
Formate	1594	v _{as} (O-C-O)
	1096,1157	v _(CO) of terminal of bridged- OCH ₃
Methane	3019	v(CH)

(3) Infrared band assignments of the surface species on ReO_x/CeO₂-P.

Surface species	Wavenumber (cm ⁻¹)	assignment
Carbonate	1398	v _s (O-C-O)
	1512	v _{as} (O-C-O)
Carboxylate	1289	v _s (O-C-O)
	2007	linearly bound
CO bond	1892	bridge bound
	2948, 2853	v(CH)
Formate	1617,1594	v _{as} (O-C-O)
	1096	v _(CO) of terminal of bridged-OCH ₃
Methane	3019	v(CH)

